高等学校化学学报
CHEMICAL JOURNAL OF CHINESE UNIVERSITIES
研究论文

原位多重光学监测的本体聚合

张瑞庆，尹　扩，陈燕杰，顾　凡，刘　健，马　骧
（华东理工大学化学与分子工程学院，上海 200237）

摘要　光学可视化是一种高灵敏度、非侵入且简便的原位监测本体聚合过程的方法. 本文合成了一种基于9,14-二苯基-9,14-二氢二苯并[a,c]吩嗪（DPAC）的分子，利用其在不同微环境下独特的激发态构象响应能够监测体系内的微观动态变化. 在甲基丙烯酸甲酯（MMA）聚合过程中，体系从液态单体逐渐转变为固态聚合物. 伴随这一过程，DPAC的荧光从红色转变为蓝色，反映了局部黏度增加与分子运动受限；随后，磷光逐渐增强且寿命延长，表明聚合物网络刚性逐步上升. 通过基于比率荧光与磷光的双通道监测，该策略实现了本体聚合过程的可视化追踪.

关键词　原位监测；本体聚合；振动诱导发光
中图分类号　O626　　**文献标志码**　A　　doi：10.7503/cjcu20260051

In situ Multiple Optical Monitoring of Bulk Polymerization

ZHANG Ruiqing，YIN Kuo，CHEN Yanjie，GU Fan，LIU Jian*，MA Xiang
（*School of Chemistry and Molecular Engineering*，*East China University of Science and Technology*，*Shanghai* 200237，*China*）

Abstract　Optical visualization provides a highly sensitive，non-invasive，and straightforward approach for the *in situ* monitoring of bulk polymerization processes. This paper synthesized a 9，14-diphenyl-9，14-dihydrodibenzo[a，c]phenazine（DPAC）-based molecule，whose distinct excited-state conformational responses under different micro-environments enabled the monitoring of microscopic dynamic changes within the system. During the polymerization of methyl methacrylate（MMA），the system transfer from a liquid monomer to a solid polymer. Accompanying this process，the fluorescence of DPAC shifts from red to blue，reflecting the increase in local viscosity and the restriction of molecular motion. Subsequently，the gradual enhancement of phosphorescence and the extension of its lifetime indicate the rising rigidity of the polymer network. Through dual-channel monitoring based on ratio-metric fluorescence and phosphorescence，this strategy makes the visual tracking of bulk polymerization feasible.

Keywords　*In situ* monitoring；Bulk polymerization；Vibration-induced emission

1　Introduction

Bulk polymerization，as a classical polymerization technique，is widely utilized in the production of polymeric materials[1]，such as coatings[2]，sprays[3]，polymer parts manufacturing[4—6]，and 3D printing[7]. During the process，the system undergoes a transition from a liquid monomer to a solid glassy polymer[8]. Despite its broad applicability，monitoring this process remains challenging：sudden acceleration of the reaction，known

收稿日期：2026-01-28. 网络首发日期：2026-03-09.
联系人简介：刘　健，男，博士，主要从事高分子化学、光功能染料和光催化等方面的研究. E-mail：liujianecust@ecust.edu.cn
基金项目：国家自然科学基金（批准号：22125803，22308102，T2488302）和广西壮族自治区科学技术厅项目（批准号：AA23062016）资助.
Supported by the National Natural Science Foundation of China（Nos.22125803，22308102，T2488302）and the Guangxi Department of Science and Technology，China（No.AA23062016）.

as the Trommsdorff effect, can occur during bulk polymerization[9], complicating precise and effective monitoring with conventional methods. Polymerization is a dynamic process, and traditional monitoring often requires disruptive sample preparation, which perturbs the system's dynamic equilibrium and native state[10]. Additionally, the continuous change in relative concentrations of monomer and polymer demands real-time, *in situ*, and non-invasive monitoring[8]. While luminescent systems have shown remarkable potential for dynamic visualization due to their optical properties[11—14], reports on luminescence-based visual monitoring of bulk polymerization remain relatively scarce.

The vibration-induced emission (VIE) and phosphorescence of the 9, 14-diphenyl-9, 14-dihydrodibenzo [a, c]phenazine (DPAC) allow real-time tracking of the increasing constraint and rigidity in the local environment during polymerization, thereby reflecting changes in molecular weight, backbone architecture, conformation, and aggregation state[15—18]. The liquid-to-glassy-solid transition in the bulk polymerization of methyl methacrylate is identified by the VIE response[19], whereas the subsequent progressive rigidification of the glassy matrix is detected through phosphorescence enhancement. This combination of ratio-metric fluorescence and phosphorescence enables visual monitoring across the entire polymerization process (Scheme 1).

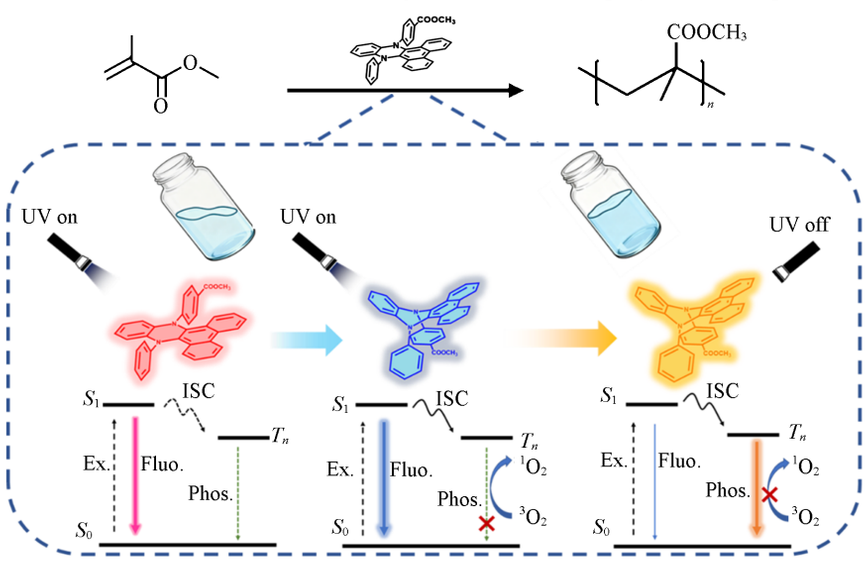

Scheme 1 Schematic diagram of *in situ* monitoring MMA polymerization

Owing to its distinctive spatial conformation, the DPAC molecule exhibits high sensitivity to micro-environmental changes[20—25]. In solution, upon photoexcitation, the molecule undergoes a conformational transition from a twisted ground state to a planar excited state, leading to extended π-conjugation and resulting in red fluorescence with a large Stokes shift. In the aggregated state, physical constraints restrict molecular motion, thereby suppressing excited-state planarization and yielding intrinsic blue fluorescence[26—28]. Furthermore, the presence of an ester group promotes efficient intersystem crossing[29], which generates phosphorescence emission in rigid environments. Consequently, this molecule can reflect the microscopic constraints within the polymerization system through its double emission modes, enabling visualization of the entire bulk polymerization process.

2 Experimental

2.1 Synthesis of DPAC

DPAC was synthesized as a luminescent molecule exhibiting double emission behaviors (Fig.S1, see the supporting information of this paper). Methyl methacrylate (MMA) was selected as the polymerization monomer.

By dissolving and doping DPAC into MMA, its emission was directly linked to real-time changes in the micro-environment of the polymer system, covering the transition from the liquid to the glassy state. During the polymerization of MMA, the increasing network rigidity progressively alters the local environment around the DPAC molecules, leading to a fluorescence wavelength change from 420 nm to 580 nm, followed by the gradual emergence of phosphorescence with enhanced intensity and extended lifetime, alongside a concurrent decrease in photoactivation. This approach enables full-process visual monitoring of polymerization through the VIE-active molecule.

2.2 Monitoring of the Polymerization Process

Bulk polymerization is a free-radical process in which monomers are polymerized with a small amount of initiator[30]; radicals act as the active centers, yielding high-purity products without the need for post-processing. However, the accompanying increase in system viscosity and solid-state glassification make real-time monitoring challenging. Owing to DPAC's unique butterfly-like conformation, this molecule can adopt either twisted or planar configurations in the excited state, exhibiting multi-color fluorescence that reflects its external environment. In solution, it displays dual emission at 420 and 580 nm. The intensity ratio of these two emission bands changes as polymerization proceeds, and only the blue emission at 420 nm remains in the glassy state. Inspired by the unique photoluminescent properties of DPAC, 0.3%(mass fraction) DPAC was added into MMA monomer, enabling real-time *in situ* monitoring of the entire bulk polymerization process of MMA.

Polymerization of MMA was selected as a model system for thermally initiated bulk polymerization due to its representativeness in free-radical bulk polymerization[31]. The DPAC molecule was designed and synthesized, and its structure was confirmed by ^{1}H NMR, ^{13}C NMR, and electrospray ionization(ESI) high-resolution mass spectrometry(Fig.S2—Fig.S4, see the supporting information of this paper). Thermally initiated free-radical polymerization was conducted in a 5 mL glass vial containing 2 mL of methyl methacrylate as monomer and 0.5%(mass fraction) azobisisobutyronitrile as initiator. The mixture was heated at 75 ℃ for 12 min for thermal activation, followed by isothermal polymerization at 45 ℃. By using ^{1}H NMR, conversion rates at different polymerization times were calculated by comparing the peak area of the characteristic polymer hydrogen(δ = 3.602) with that of the monomer hydrogen(δ = 3.75). Weight-average molecular weights were determined by gel permeation chromatography, confirming the time-dependent nature of the polymerization.

3 Results and Discussion

3.1 Fluorescence Monitoring of Polymerization Processes

The visualization mechanism during the bulk polymerization of MMA was investigated. Since MMA itself serves as a good solvent for the luminescent molecule, DPAC was directly added in the monomer. The doped DPAC exhibited typical dual-wavelength emission, whose intensity changed significantly with the reaction process[Fig.1(A)]. As shown in Figs.1(B) and (F), corresponding changes were also visually observed in the fluorescence photographs of the polymer, which were consistent with our spectroscopic measurements. These variations were clearly illustrated by the CIE chromaticity diagram, laying a foundation for the visualization of the polymerization process.

We further examined the effect of increasing viscosity during polymerization on the fluorescence properties of the DPAC unit[Figs.1(A) and (E), Fig.S5(see the supporting information of this paper)]. Parallel experiments were conducted with polymerization times ranging from 0 to 7 h to control chain length and thus modulate chain conformation. In the MMA monomer, the system is in a solution state. With the polymerization proceeding, the viscosity gradually increases and the system transfer into a glassy state. This progressively enhances the

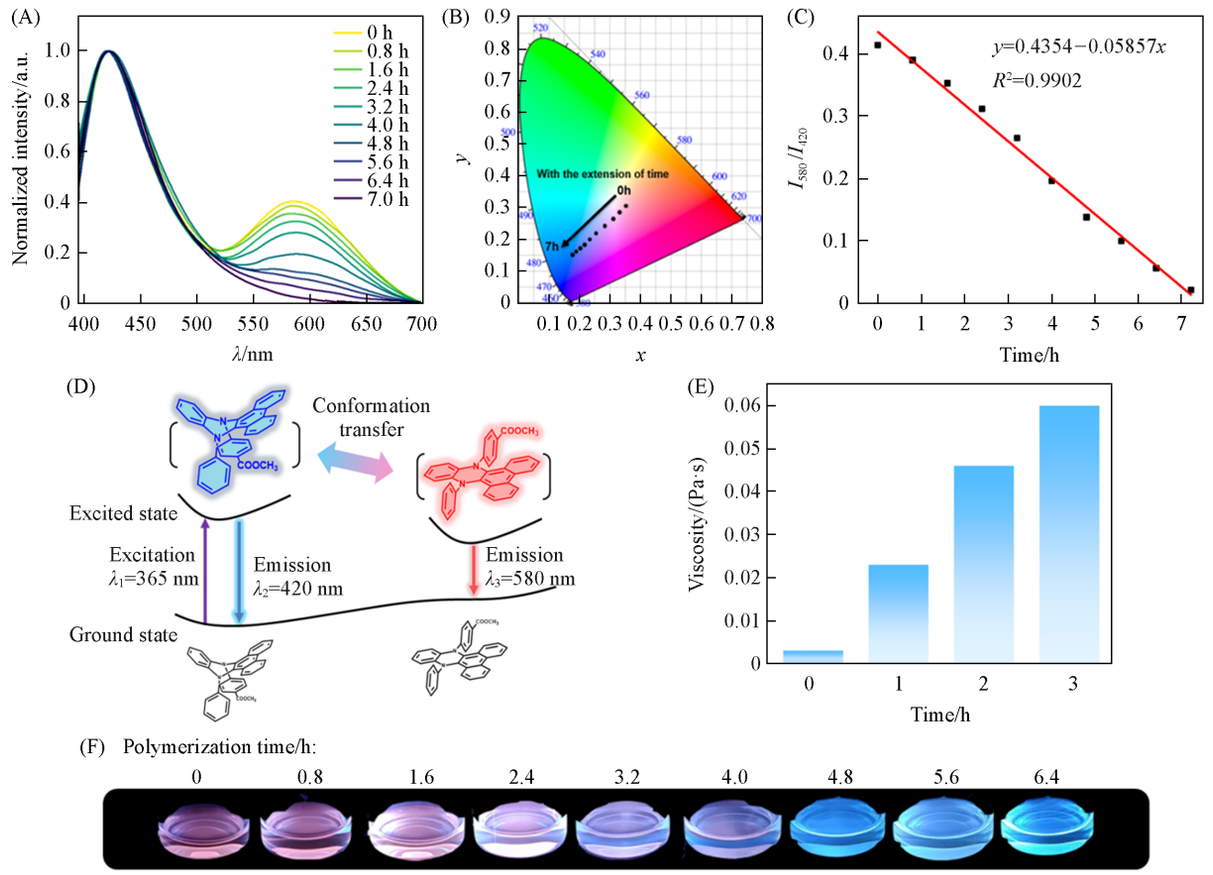

Fig. 1 Fluorescent *in situ* monitoring of MMA polymerization

(A) Fluorescence spectra of PMMA during the first 7 h; (B) CIE diagram coordinate shifting as time; (C) normalized curve of fluorescence intensity at 580 nm over time; (D) energy landscape of the excited-state conformational transfer of DPAC units to emit dual-wavelength fluorescence under different confinement; (E) viscosity of PMMA changes over time; (F) photographs of the polymerization process.

constraints on the DPAC molecules, affecting their conformation and ultimately leading to changes in fluorescence behavior. By normalizing the peak at 420 nm, we obtained the curve of the peak at 580 nm changing over time. Thus, we have developed a ratio metric fluorescent molecule based on these properties for monitoring polymerization processes [Fig. 1(C)]. The color change of this ratio metric fluorescent molecule originates from the increasing viscosity as free monomers polymerize into long-chain polymers, which suppresses the excited-state planarization process [Fig.1(D), Fig. S6(see the supporting information of this paper)].

3.2 Phosphorescence Monitoring of Polymerization Processes

After the polymerization system reached the glassy state at 7 h, the fluorescence emission of the DPAC unit no longer showed significant changes. However, we observed that the polymer system exhibited distinct afterglow behavior [Fig.2(A)], and the afterglow duration gradually lengthened with the progression of polymerization.

Subsequently, we further examined the capability of this molecule for monitoring the glassy-state bulk polymerization process. Parallel experiments were conducted with polymerization times ranging from 7 h to 14 h. As polymer chain length increased, the afterglow duration visible in photographs gradually lengthened [Fig.2(G)]. Delayed emission spectra confirmed the emergence of phosphorescence around 550 nm, which intensified with polymerization progress, while the phosphorescence lifetime increased from the initial 22.41 ms to 271.85 ms, then we fitted curves of lifetime and intensity over time [Figs.2(A) and (B), Fig S7(see the

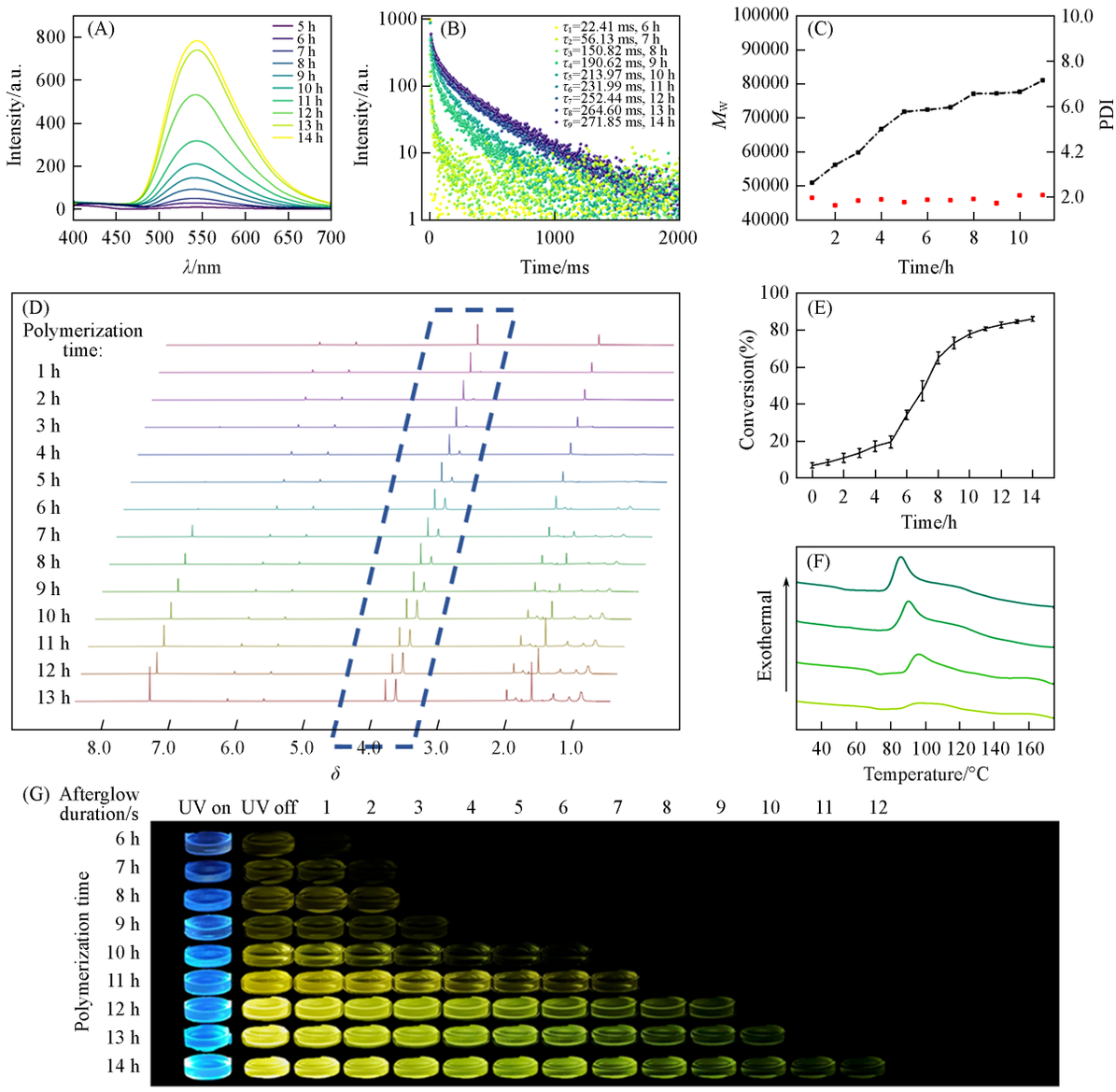

Fig. 2 Phosphorescence *in situ* monitoring of MMA polymerization

(A) Phosphorescence intensity variation from 5 h to 14 h; (B) lifetime spectra at different times; (C) variation curves of M_w and polymer dispersity index(PDI) with time; (D) NMR spectra corresponding to various polymerization times; (E) conversion *versus* time curve with error bars; (F) DSC *versus* time curves during the polymerization process; (G) afterglow photos during polymerization.

supporting information of this paper)]. The polymerization of MMA was characterized by GPC and ^{1}H NMR spectroscopy[Figs.2(C) and (D)], and the time-dependent monomer conversion was calculated, which confirm the time-dependent nature of the polymerization[Fig.2(E)]. Our hypothesis was supported by differential scanning calorimetry measurements[Fig.2(F)], the glass-transition temperature of PMMA increases from 56 ℃ to 78 ℃, confirming that the enhancement of phosphorescence originates from the increased network rigidity of PMMA.

3.3 Photoactivated Monitoring of Polymerization Processes

Upon UV irradiation, the luminescence of the polymer system gradually increased; however, this photoactivation effect continuously diminished as polymerization advanced. Samples with different polymerization time were selected to characterize the photoactivation behavior. For the 8 h sample, the phosphorescence intensity was only 19 without photoactivation, but increased to 662 after 10 s of UV irradiation, corresponding

to a 33-fold enhancement[Fig.3(A_1)]. Parallel experiments on the 10, 12, and 14 h samples revealed that the 10 h sample showed a 18-fold increase after 20 s of photoactivation, while the 14 h sample exhibited only a 1.3-fold increase after 50 s, indicating a clear decline in photoactivation efficiency, as visually depicted in Figs.3(A_2)—(A_4) and (C). Phosphorescence lifetime measurements performed on the four groups showed a similar trend. Taking the 8 h sample as an example, its phosphorescence lifetime increased from an initial 2.69 ms to 150.82 ms after 10 s of photoactivation, representing a 56-fold extension[Figs.3(B_1)—(B_4) and (D). As polymerization time increased, the influence of photoactivation on lifetime became less pronounced.

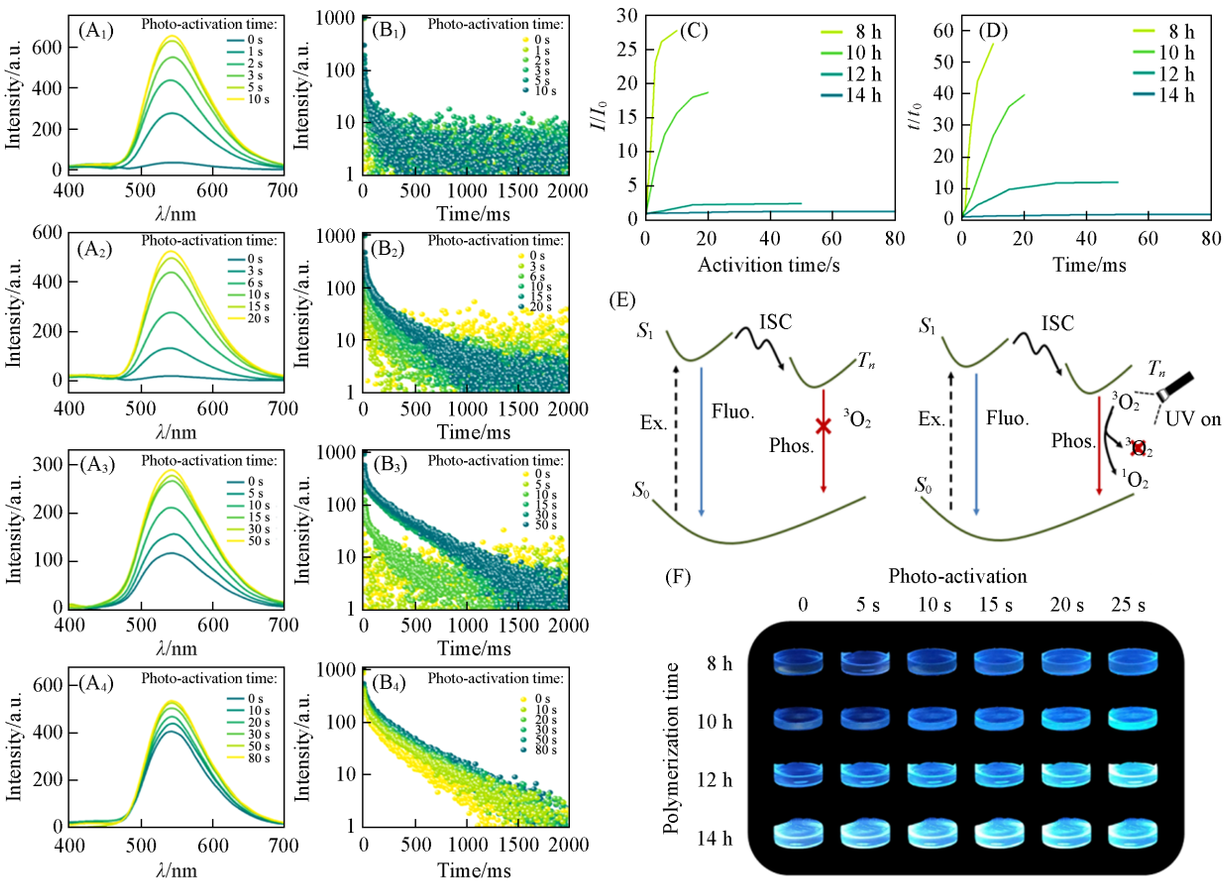

Fig. 3 Photoactivation *in situ* monitoring of MMA polymerization

(A_1—A_4) Photoactivated phosphorescence spectra at 8 h(A_1), 10 h(A_2), 12 h(A_3), 14 h(A_4) of polymerization; (B_1—B_4) photoactivated lifetime spectra at 8 h(B_1), 10 h(B_2), 12 h(B_3), 14 h(B_4) of polymerization; (C) phosphorescence intensity change rate *versus* time curves; (D) phosphorescence lifetime change rate *versus* time curves; (E) diagram of photoactivation mechanism; (F) photographs after photoactivation.

This photoactivation phenomenon arises from residual oxygen trapped within the polymer matrix. Ground-state triplet oxygen quenches the phosphorescence of DPAC; under UV light, oxygen is excited to the singlet state, thereby suppressing quenching and enhancing phosphorescence emission[Fig.3(E)]. Advancement of the reaction process increases the compactness of the matrix, which impedes oxygen permeation. Therefore, the extent of photoactivation can serve as an indicator for *in situ* monitoring of MMA bulk polymerization[Fig.3(F)]. During the glassy-state polymerization, the oxygen-blocking ability of the polymer progressively improves, accompanied by a distinct weakening of photoactivation.

4 Conclusions

By employing an ester-functionalized DPAC molecule in the bulk polymerization of MMA and exploiting

its excited-state conformational dynamics, we achieved *in situ* monitoring of the entire polymerization process. This work effectively combines fluorescence and phosphorescence, utilizing changes in optical behavior to reveal intrinsic polymer properties and thereby addressing the challenge of real-time dynamic monitoring in bulk polymerization. The non-invasive and highly sensitive nature of this strategy enables real-time observation of polymerization effects. It offers a straightforward monitoring approach for the polymerization industry and provides a new perspective for the application of optical materials.

The supporting information of this paper see http://www.cjcu.jlu.edu.cn/CN/10.7503/cjcu20260051.

References

[1] Awaja F., Gilbert M., Kelly G., Fox B., Pigram P. J., *Prog. Polym. Sci.*, **2009**, *34*(9), 948—968
[2] Jin F. L., Li X., Park S. J., *J. Ind. Eng. Chem.*, **2015**, *29*, 1—11
[3] Breschi L., Mazzoni A., Ruggeri A., Cadenaro M., Lenarda Di R., de Stefano Dorigo E., *Dent. Mater.*, **2008**, *24*(1), 90—101
[4] Rijswijk van K., Bersee H. E. N., *Compos. Part A: Appl. Sci. Manuf.*, **2007**, *38*(3), 666—681
[5] Suzuki Y., Mishima R., Matsumoto A., *Int. J. Chem. Kinet.*, **2022**, *54*(6), 361—370
[6] Robertson I. D., Yourdkhani M., Centellas P. J., Aw D. G., Ivanoff J. E., Goli E., Lloyd E. M., Dean L. M., Sottos N. R., Geubelle P. H., Moore J. S., White S. R., *Nature*, **2018**, *557*(7704), 223—227
[7] Murray R. E., Penumadu D., Cousins D., Beach R., Snowberg D., Berry D., Suzuki Y., Stebner A., *Appl. Compos. Mater.*, **2019**, *26*(3), 945—961
[8] Jessen L. L., Hansen K. R., Crull G. B., Grover T. L., Guymon C. A., *ACS Macro Lett.*, **2025**, *14*(6), 847—852
[9] Trommsdorff V. E., Köhle H., Lagally P., *Makromol. Chem.*, **2003**, *1*(3), 169—198
[10] Leira-Iglesias J., Tassoni A., Adachi T., Stich M., Hermans T. M., *Nat. Nanotechnol.*, **2018**, *13*(11), 1021—1027
[11] Gao C., Silvi S., Ma X., Tian H., Credi A., Venturi M., *Chem.-Eur. J.*, **2012**, *18*(52), 16911—16921
[12] Chen H., Yao X. Y., Ma X., Tian H., *Adv. Opt. Mater.*, **2016**, *4*(9), 1397—1401
[13] Zhang D., Su J. H., Ma X., Tian H., *Tetrahedron*, **2008**, *64*(36), 8515—8521
[14] Sun J., Huang Z. Z., He Z. Y., Hu Y., Li C. L., Wu Z. Q., Tian H., Ma X., *Adv. Opt. Mater.*, **2026**, *14*, e03796
[15] Zhang Z. Y., Wu Y. S., Tang K. C., Chen C. L., Ho J. W., Su J. H., Tian H., Chou P. T., *J. Am. Chem. Soc.*, **2015**, *137*(26), 8509—8520
[16] Zheng S. D., Ma M. Y., Qu D. H., Tian H., Zhang Q., *Angew. Chem. Int. Ed.*, **2025**, *64*(34), e202507770
[17] Ding B. B., Ma X., Tian H., *Acc. Mater. Res.*, **2023**, *4*(10), 827—838
[18] Gu F., Jiang T., Ma X., *ACS Appl. Mater. Interfaces*, **2021**, *13*(36), 43473—43479
[19] Mori N., Matsumoto A., Suzuki Y., *Macromolecules*, **2025**, *58*(9), 4699—4707
[20] Chen W., Chen C. L., Zhang Z. Y., Chen Y. A., Chao W. C., Su J. H., Tian H., Chou P. T., *J. Am. Chem. Soc.*, **2017**, *139*(4), 1636—1644
[21] Humeniuk H. V., Rosspeintner A., Licari G., Kilin V., Bonacina L., Vauthey E., Sakai N., Matile S., *Angew. Chem. Int. Ed.*, **2018**, *57*(33), 10559—10563
[22] Sun G. C., Pan J. J., Wu Y. F., Liu Y., Chen W., Zhang Z. Y., Su J. H., *ACS Appl. Mater. Interfaces*, **2020**, *12*(9), 10875—10882
[23] Wang J., Yao X. Y., Liu Y., Zhou H. T., Chen W., Sun G. C., Su J. H., Ma X., Tian H., *Adv. Opt. Mater.*, **2018**, *6*, 1800074
[24] Wang H., Li Y. R., Zhang Y. Y., Mei J., Su J. H., *Chem. Commun.*, **2019**, *55*(13), 1879—1882
[25] Huang W., Sun L., Zheng Z. W., Su J. H., Tian H., *Chem. Commun.*, **2015**, *51*(21), 4462—4464
[26] Zhou H. T., Mei J., Chen Y. A., Chen C. L., Chen W., Zhang Z. Y., Su J. H., Chou P. T., Tian H., *Small*, **2016**, *12*(47), 6542—6546
[27] Zhang Z. Y., Song W. X., Su J. H., Tian H., *Adv. Funct. Mater.*, **2019**, *30*(2), 1902803
[28] Sun G. C., Zhou H. T., Liu Y., Li Y. R., Zhang Z. Y., Mei J., Su J. H., *ACS Appl. Mater. Interfaces*, **2018**, *10*(23), 20205—20212
[29] Hirata S., Kamatsuki T., *J. Phys. Chem. C*, **2023**, *127*(7), 3861—3871
[30] Silva J. S., Melo P. A., Pinto J. C., *Macromol. React. Eng.*, **2023**, *17*(4), 2300001
[31] Nölle J. M., Primpke S., Müllen K., Vana P., Wöll D., *Polym. Chem.*, **2016**, *7*(24), 4100—4105

(Ed.: Y, K, M)